Supplementary Material

Section 1. Supplementary Figures and Tables

Table A1. Estimated time until COVID-19 hospitalizations exceed local hospital bed surge capacity and cumulative COVID-19 hospitalizations and deaths for the Austin-Round Rock MSA from February 16 through December 31, 2020, assuming that social distancing measures are relaxed on May 1, 2020. The values are medians (with 95% range in parentheses) across 200 stochastic simulations based on the parameters given in Appendix. Entries with *NE* are not expected to surpass the specified thresholds prior to December 31, 2020.

Transmission reduction after May 1st relaxation	With cocooning			Without cocooning		
	Days to exceed surge capacity	Cumulative hospital beds	Cumulative deaths	Days to exceed surge capacity	Cumulative hospital beds	Cumulative deaths
0%	46 (37 - 56)	35,000 (33,906 - 36,219)	3,181 (3,027 - 3,366)	29 (19 - 44)	90,488 (89,969 - 91,006)	11,670 (11,498 - 11,862)
50%	81 (59 - 111)	34,414 (33,109 - 35,575)	3,108 (2,934 - 3,313)	51 (38 - 81)	86,560 (85,609 - 87,288)	10,847 (10,634 - 11,101)
75%	NE	23,938 (7,367 - 28,585)	1,907 (457 - 2,501)	109 (72 - 184)	67,611 (44,578 - 70,850)	7,552 (3,980 - 8,172)
85%	NE	2,044 (117 - 8,858)	158 (6 - 786)	NE	9,141 (1,826 - 27,407)	795 (136 - 2625)
90%	NE	725 (29 - 3,307)	74 (0 - 348)	NE	1,239 (62 - 4,670)	128 (9 - 459)

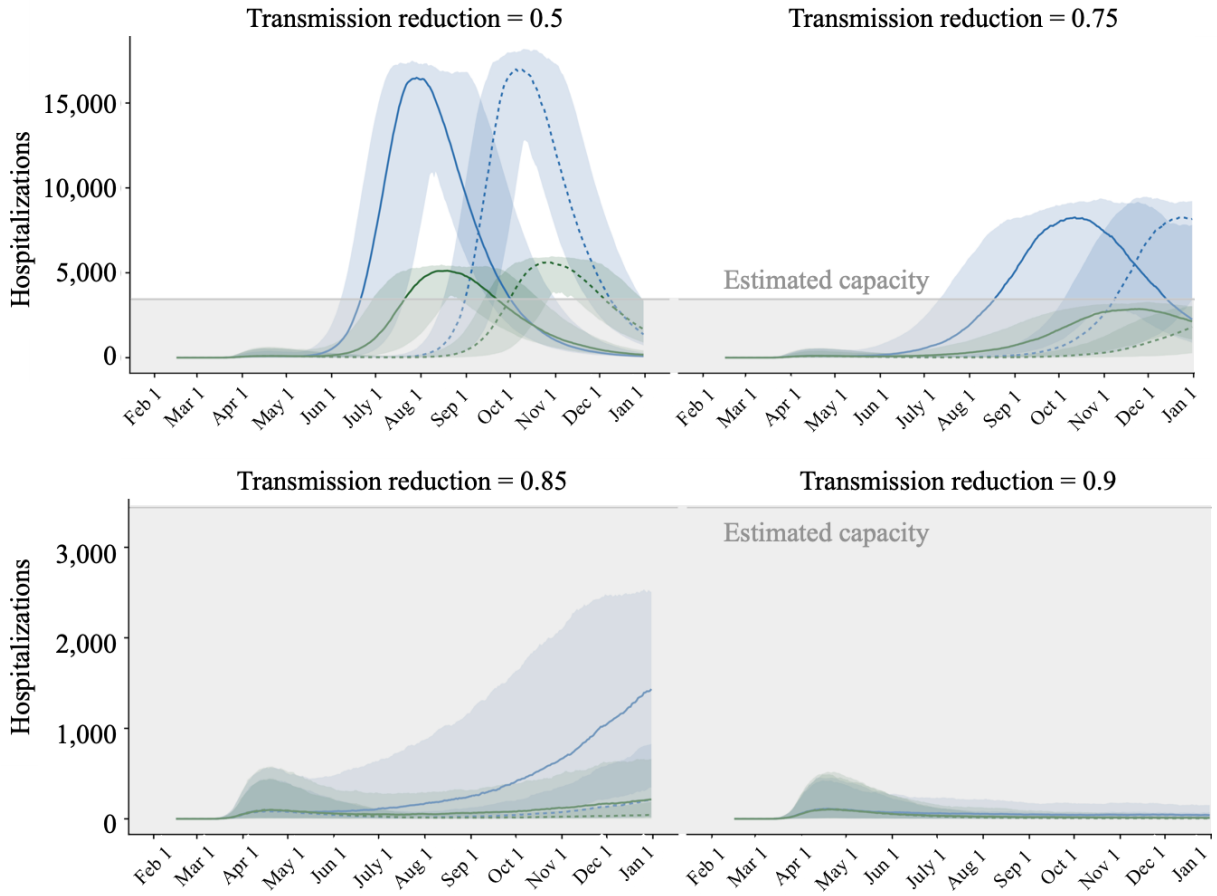

Figure A1. Projected daily COVID-19 hospitalizations in the Austin-Round Rock MSA from February 16 to December 31, 2020 coupled with different degrees of transmission reduction after the relaxation of the *Stay Home-Work Safe* order on either May 1 (solid lines), or July 1 (dashed lines). Prior to May 1, we estimate that social distancing has reduced transmission by 95% relative to the baseline prior to the March 15th closure of schools in Austin. After May 1, we consider relaxation scenarios in which transmission is reduced by only 50% (top left), 75% (top right), 85% (bottom left), and 90% (bottom right). The green lines assume cocooning of vulnerable populations, that is, everyone over 65 and others with high-risk comorbidities continue to social distance and take precautions that reduce their risk of infection by 95%. The blue lines project COVID-19 cases assuming that these vulnerable populations instead have the same transmission reduction as the rest of the population. Lines and shading indicate the median and 95% prediction interval across 200 stochastic simulations.

Section 2. Stochastic Compartmental Model of COVID-19 Transmission in the Austin-Round Rock Metropolitan Area

The model structure is diagrammed in Figure A2 and described in the equations below.
For each age and risk group, we build a separate set of compartments to model the transitions between the states: susceptible (S), exposed (E), symptomatic infectious (I^Y), asymptomatic infectious (I^A), symptomatic infectious that are hospitalized (I^H), recovered (R), and deceased (D). The symbols S, E, I^Y, I^A, I^H, R, and D denote the number of people in that state in the given age/risk group and the total size of the age/risk group is $N = S + E + I^Y + I^A + I^H + R + D$.
The model for individuals in age group a and risk group r is given by:

$$\frac{dS_{a,r}}{dt} = -\sum_{i\in A}\sum_{j\in K}(I^Y_{i,j}\omega^Y + I^A_{i,j}\omega^A + E_{i,j}\omega^E)(1-\kappa)\beta\phi_{a,i}/N_i$$

$$\frac{dE_{a,r}}{dt} = \sum_{i\in A}\sum_{j\in K}(I^Y_{i,j}\omega^Y + I^A_{i,j}\omega^A + E_{i,j}\omega^E)(1-\kappa)\beta\phi_{a,i}/N_i - \sigma E_{a,r}$$

$$\frac{dI^A_{a,r}}{dt} = (1-\tau)\sigma E_{a,r} - \gamma^A I^A_{a,r}$$

$$\frac{dI^Y_{a,r}}{dt} = \tau\sigma E_{a,r} - (1-\pi)\gamma^Y I^Y_{a,r} - \pi\eta I^Y_{a,r}$$

$$\frac{dI^H_{a,r}}{dt} = \pi\eta I^Y_{a,r} - (1-\nu)\gamma^H I^H_{a,r} - \nu\mu I^H_{a,r}$$

$$\frac{dR_{a,r}}{dt} = \gamma^A I^A_{a,r} + (1-\pi)\gamma^Y I^Y_{a,r} + (1-\nu)\gamma^H I^H_{a,r}$$

$$\frac{dD_{a,r}}{dt} = \nu\mu I^H_{a,r}$$

where A and K are all possible age and risk groups, ^{A}, ^{Y}, ^{H} are relative infectiousness of the I^A, I^Y, E compartments, respectively, β is transmission rate, κ is the transmission rate multiplier that models the reduction in transmission resulting from social distancing, $_{a,i}$ is the mixing rate between age group a, $i \in A$, ^{A}, ^{Y}, ^{H} are the recovery rates for the I^A, I^Y, I^H compartments, respectively, σ is the exposed rate, τ is the symptomatic ratio, π is the proportion of symptomatic individuals requiring hospitalization, η is rate at which hospitalized cases enter the hospital following symptom onset, ν is mortality rate for hospitalized cases, and μ is rate at which terminal patients die.

We model stochastic transitions between compartments using the τ-leap method (1,2) with key parameters given in Table S1. Assuming that the events at each time-step are independent and do not impact the underlying transition rates, the numbers of each type of event should follow Poisson distributions with means equal to the rate parameters. We thus simulate the model according to the following equations:

$$S_{a,r}(t+1) - S_{a,r}(t) = -P_1$$

$$E_{a,r}(t+1) - E_{a,r}(t) = P_1 - P_2$$

$$I^A_{a,r}(t+1) - I^A_{a,r}(t) = (1-\tau)P_2 - P_3$$

$$I^Y_{a,r}(t+1) - I^Y_{a,r}(t) = \tau P_2 - P_4 - P_5$$

$$I^H_{a,r}(t+1) - I^H_{a,r}(t) = P_5 - P_6 - P_7$$

$$R_{a,r}(t+1) - R_{a,r}(t) = P_3 + P_4 + P_6$$

$$D_{a,r}(t+1) - D_{a,r}(t) = P_7,$$

with

$$P_1 \sim \text{Pois}(S_{a,r}(t)F_{a,r}(t))$$
$$P_2 \sim \text{Pois}(\sigma E_{a,r}(t))$$
$$P_3 \sim \text{Pois}(\gamma^A I^A_{a,r}(t))$$
$$P_4 \sim \text{Pois}((1-\pi)\gamma^Y I^Y_{a,r}(t))$$
$$P_5 \sim \text{Pois}(\pi\eta I^Y_{a,r}(t))$$
$$P_6 \sim \text{Pois}((1-\nu)\gamma^H I^H_a)$$
$$P_7 \sim \text{Pois}(\nu\mu I^H_{a,r}(t))$$

and where $F_{a,r}$ denotes the force of infection for individuals in age group a and risk group r and is given by:

$$F_{a,r}(t) = \sum_{i\in A}\sum_{j\in K}(I^Y_{i,r}(t)\omega^Y + I^A_{i,r}(t)\omega^A + E_{i,j}(t)\omega^E)(1-\kappa)\beta_{a,i}\phi_{a,i}/N_i$$

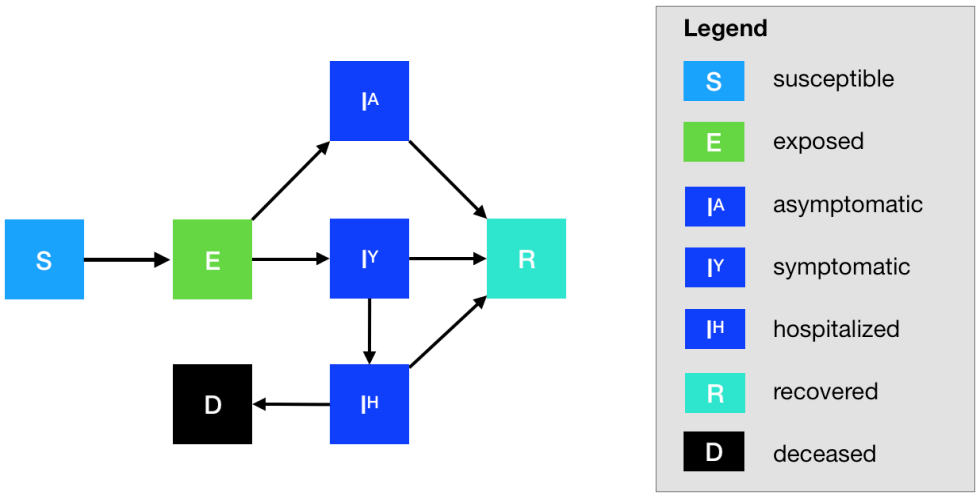

Figure A2. Compartmental model of COVID-19 transmission in a US city. Each subgroup (defined by age and risk) is modeled with a separate set of compartments. Upon infection, susceptible individuals (S) progress to exposed (E) and then to either symptomatic infectious (I^Y) or asymptomatic infectious (I^A). All asymptomatic cases eventually progress to a recovered class where they remain protected from future infection (R); symptomatic cases are either hospitalized (I^H) or recover. Mortality (D) varies by age group and risk group and is assumed to be preceded by hospitalization.

Parameter Estimation

Table A2. COVID-19 hospitalizations in Austin-Round Rock MSA from March 13, 2020 to April 24, 2020

Date	Hospitalized	Date	Hospitalized	Date	Hospitalized
3/13/20	1	3/28/20	29	4/11/20	76
3/14/20	1	3/29/20	32	4/12/20	75
3/15/20	1	3/30/20	41	4/13/20	81
3/16/20	1	3/31/20	44	4/14/20	82
3/17/20	1	4/1/20	52	4/15/20	80
3/18/20	1	4/2/20	56	4/16/20	80
3/19/20	5	4/3/20	57	4/17/20	79
3/20/20	7	4/4/20	63	4/18/20	78
3/21/20	6	4/5/20	65	4/19/20	79
3/22/20	9	4/6/20	69	4/20/20	83
3/23/20	10	4/7/20	69	4/21/20	78
3/24/20	17	4/8/20	70	4/22/20	82
3/25/20	22	4/9/20	71	4/23/20	78
3/26/20	25	4/10/20	75	4/24/20	75
3/27/20	25				

Parameter estimation using Austin hospitalization data

The city of Austin provided the total number of *heads in beds* for confirmed COVID-19 patients in hospitals in Austin-Round Rock MSA from March 13 to April 24, 2020 (Table A2). Let $H(t)$ and $\hat{H}(t)$ be the observed and predicted hospitalization totals on day t, where predictions are made from the deterministic model formulation. We conducted least-squares fitting to estimate β, κ, and t_0, corresponding to the baseline transmission rate, the reduction in contacts following Austin's Stay Home-Work Safe Order, and the initial seed date of the epidemic respectively. Fitting was conducted using the nonlinear least squares method made available in scipy, which minimizes the least squares error defined as $\mathrm{LSE} = (H(t) - \hat{H}(t))^2$ (3). The best fit model accurately captured the hospitalization data and estimated $\hat{\beta} = 0.035$, $\hat{\kappa} = 0.95$, and $\hat{t_0} = \text{February } 16, 2020$.

We calculated 95% confidence intervals for $\hat{\kappa}$ by comparing prediction intervals from stochastic simulations with the hospitalization data. We ran 500 stochastic simulations for each of the following possible values of κ': 0.0, 0.05, ..., 0.95, 1.0. For each value of κ', we conducted the following analysis to determine if κ' lies inside the 95% confidence interval for $\hat{\kappa}$.

- For all simulations, we calculate the day-to-day difference in hospitalizations (i.e., heads in beds) during the period following the *Stay Home-Work Safe* order: $\hat{z}_t = \hat{H}_t - \hat{H}_{t-1}$. We do the same for the actual data: $z_t = H_t - H_{t-1}$.
- We compute the 95% prediction interval for $\hat{z}_t$ across all 500 stochastic simulations for κ' for each day t
- We then conduct a test of the null hypothesis $H_0 : \kappa' = \kappa$. Under this null hypothesis, we would expect roughly 95% of the observed data (z_t) to fall within the 95% prediction band for $\hat{z}_t$ that we constructed from our simulations. By analyzing the day-to-day difference in hospitalizations rather than daily hospitalizations, we can assume that the data are independent from one day to the next. Then the expected number of observed values contained in the 95% prediction band is given by the binomial expression:

  $$N_{\text{observed}} \sim B\left(N_{\text{points}}, 0.95\right)$$

  where N_{observed} is the number of data points contained within the 95% prediction band and N_{points} is the total number of data points (i.e., days).
- We calculate $N_{\text{contained}}$, the actual number of data points contained within the 95% prediction band, and compute a p-value by identifying the probability that one would observe $N_{\text{contained}}$ or more extreme results under the null distribution. If p<0.05, we reject the null hypothesis $H_0 : \kappa' = \kappa$.

Model Parameters

Table A3. Initial conditions, school closures and social distancing policies

Variable	Settings
Initial day of simulation	2/16/2020
Initial infection number in locations	1 symptomatic case in 18-49y age group
School closure	3/15/2020 - 8/17/2020
Age-specific and day-specific contact rates	Home, work, other and school matrices provided in Tables A6.1-A6.4 ● From 2020-02-16 to 2020-03-18 Weekday = home + school + work + other Weekend = home + other Weekday holiday = home + other ● From 2020-03-19 to 2020-03-24 Weekday = home + work + other Weekend = home + other Weekday holiday = home + other ● From 2020-03-25 to 2020-08-17 Weekday = (1-κ)*(home + work + other) Weekend = (1-κ)*(home + other) Weekday holiday = (1-κ)*(home + other) ● From 2020-08-18 to 2020-12-31 Weekday = (1-κ)*(home + school + work + other) Weekend = (1-κ)*(home + other) Weekday holiday = (1-κ)*(home + other)

Table A4. Model parameters[a]

Parameters	Values	Source
R_0: reproduction number	2.8	Derived from fitted model
δ: doubling time before intervention	2.9 days	Derived from fitted model
β: baseline transmission rate	0.035	Fitted to daily COVID-19 hospitalizations in Austin-Round Rock MSA
κ: reduction in transmission	From 2020-02-15 to 2020-03-24: 0 From 2020-03-25 to 2020-05-01: 0.95 [95% CI: 0.7 - 1] From 2020-03-25 to 2020-12-31: 5 scenarios [0, 0.5, 0.7, 0.85, 0.95]	From 2020-03-25 to 2020-05-01: fitted to daily COVID-19 hospitalizations in Austin-Round Rock MSA
γ^A: recovery rate on asymptomatic compartment	Equal to γ^Y	

γ^Y : recovery rate on symptomatic non-treated compartment	$\frac{1}{\gamma^Y} \sim \text{Triangular}(21.2, 22.6, 24.4)$	Verity et al. (4)
τ : symptomatic proportion (%)	82.1	Mizumoto et al. (5)
σ : exposed rate	$\frac{1}{\sigma} \sim \text{Triangular}(5.6, 7, 8.2)$	Lauer et al. (6)
P: proportion of pre-symptomatic transmission (%)	12.6	Du et al. (7)
ω^E : relative infectiousness of infectious individuals in compartment E	$\omega^E = \frac{(\frac{YHR}{\eta} + \frac{1-YHR}{\gamma^Y})\omega^Y \sigma P}{1-P}$	
ω^A : relative infectiousness of infectious individuals in compartment I^A	0.4653	Set to mean of ω^E
IFR: infected fatality ratio, age specific (%)	Low risk: [0.0009, 0.0022, 0.0339, 0.2520, 0.6440] High risk: [0.0092, 0.0218, 0.3388, 2.5197, 6.4402]	Age adjusted from Verity et al. (4)
YFR: symptomatic fatality ratio, age specific (%)	Low risk: [0.0011165, 0.0027 , 0.0412, 0.3069, 0.7844] High risk: [0.0112, 0.0265, 0.4126, 3.0690, 7.8443]	$YFR = \frac{IFR}{1-\tau}$
h : high-risk proportion, age specific (%)	[8.2825, 14.1121, 16.5298, 32.9912, 47.0568]	Estimated using 2015-2016 Behavioral Risk Factor Surveillance System (BRFSS) data with multilevel regression and poststratification using CDC's list of conditions that may increase the risk of serious complications from influenza (8–10)

[a]Values given as five-element vectors are age-stratified with values corresponding to 0-4, 5-17, 18-49, 50-64, 65+ year age groups, respectively.

Table A5 Hospitalization parameters

Parameters	Value	Source
γ^H : recovery rate in hospitalized compartment	1/14	14 day-average from admission to discharge (UT Austin Dell Med)
YHR: symptomatic case hospitalization rate (%)	Low risk: [0.0279, 0.0215, 1.3215, 2.8563, 3.3873] High risk: [0.2791, 0.2146, 13.2154, 28.5634, 33.8733]	Age adjusted from Verity et al. (4)
π : rate of symptomatic individuals go to hospital, age-specific	$\pi = \frac{\gamma^Y * YHR}{\eta + (\gamma^Y - \eta)YHR}$	
η : rate from symptom onset to hospitalized	0.1695	5.9 day average from symptom onset to hospital admission Tindale et al. (11)
μ : rate from hospitalized to death	1/14	14 day-average from admission to death (UT Austin Dell Med)
HFR: hospitalized fatality ratio, age specific (%)	[4, 12.365, 3.122, 10.745, 23.158]	$HFR = \frac{IFR}{YHR(1-\tau)}$
ν : death rate on hospitalized individuals, age specific	[0.0390, 0.1208, 0.0304, 0.1049, 0.2269]	$\nu = \frac{\gamma^H HFR}{\mu + (\gamma^H - \mu)HFR}$
ICU: proportion hospitalized people in ICU	[0.15, 0.20, 0.15, 0.20, 0.15]	CDC planning scenarios (based on US seasonal flu data)
Vent: proportion of individuals in ICU needing ventilation	0.67	Assumption
d_{ICU} : duration of stay in ICU	10 days	Assumption, set equal to duration of ventilation
d_V : duration of ventilation	10 days	Assumption
Healthcare capacity	Hospital beds: 4299 (assume 80% available for COVID-19)	Estimates provided by each of the region's hospital systems and aggregated by regional public health leaders

Table A6.1 Home contact matrix. Daily number contacts by age group at home.

	0-4y	5-17y	18-49y	50-64y	65y+
0-4y	0.5	0.9	2.0	0.1	0.0
5-17y	0.2	1.7	1.9	0.2	0.0
18-49y	0.2	0.9	1.7	0.2	0.0
50-64y	0.2	0.7	1.2	1.0	0.1
65y+	0.1	0.7	1.0	0.3	0.6

Table A6.2 School contact matrix. Daily number contacts by age group at school.

	0-4y	5-17y	18-49y	50-64y	65y+
0-4y	1.0	0.5	0.4	0.1	0.0
5-17y	0.2	3.7	0.9	0.1	0.0
18-49y	0.0	0.7	0.8	0.0	0.0
50-64y	0.1	0.8	0.5	0.1	0.0
65y+	0.0	0.0	0.1	0.0	0.0

Table A6.3 Work contact matrix. Daily number contacts by age group at work.

	0-4y	5-17y	18-49y	50-64y	65y+
0-4y	0.0	0.0	0.0	0.0	0.0
5-17y	0.0	0.1	0.4	0.0	0.0
18-49y	0.0	0.2	4.5	0.8	0.0
50-64y	0.0	0.1	2.8	0.9	0.0
65y+	0.0	0.0	0.1	0.0	0.0

Table A6.4 Others contact matrix. Daily number contacts by age group at other locations.

	0-4y	5-17y	18-49y	50-64y	65y+
0-4y	0.7	0.7	1.8	0.6	0.3
5-17y	0.2	2.6	2.1	0.4	0.2
18-49y	0.1	0.7	3.3	0.6	0.2
50-64y	0.1	0.3	2.2	1.1	0.4
65y+	0.0	0.2	1.3	0.8	0.6

Section 3. Estimation of age-stratified proportion of population at high-risk for COVID-19 complications

We estimate age-specific proportions of the population at high risk of complications from COVID-19 based on data for Austin, TX and Round-Rock, TX from the CDC's 500 cities project (Figure A3) (12). We assume that high risk conditions for COVID-19 are the same as those specified for influenza by the CDC (8). The CDC's 500 cities project provides city-specific estimates of prevalence for several of these conditions among adults (13). The estimates were obtained from the 2015-2016 Behavioral Risk Factor Surveillance System (BRFSS) data using a small-area estimation methodology called multi-level regression and poststratification (9,10). It links geocoded health surveys to high spatial resolution population demographic and socioeconomic data (10).

Estimating high-risk proportions for adults. To estimate the proportion of adults at high risk for complications, we use the CDC's 500 cities data, as well as data on the prevalence of HIV/AIDS, obesity and pregnancy among adults (Table A7).

The CDC 500 cities dataset includes the prevalence of each condition on its own, rather than the prevalence of multiple conditions (e.g., dyads or triads). Thus, we use separate co-morbidity estimates to determine overlap. Reference about chronic conditions (14) gives US estimates for the proportion of the adult population with 0, 1 or 2+ chronic conditions, per age group. Using this and the 500 cities data we can estimate the proportion of the population p_{HR} in each age group in each city with at least one chronic condition listed in the CDC 500 cities data (Table A7) putting them at high-risk for flu complications.

HIV: We use the data from table 20a in CDC HIV surveillance report (15) to estimate the population in each risk group living with HIV in the US (last column, 2015 data). Assuming independence between HIV and other chronic conditions, we increase the proportion of the population at high-risk for influenza to account for individuals with HIV but no other underlying conditions.
Morbid obesity: A BMI over 40kg/m^2 indicates morbid obesity, and is considered high risk for influenza. The 500 Cities Project reports the prevalence of obese people in each city with BMI over 30kg/m^2 (not necessarily morbid obesity). We use the data from table 1 in Sturm and Hattori (16) to estimate the proportion of people with BMI>30 that actually have BMI>40 (across the US); we then apply this to the 500 Cities obesity data to estimate the proportion of people who are morbidly obese in each city. Table 1 of Morgan et al. (17) suggests that 51.2% of morbidly obese adults have at least one other high risk chronic condition, and update our high-risk population estimates accordingly to account for overlap.
Pregnancy: We separately estimate the number of pregnant women in each age group and each city, following the methodology in CDC reproductive health report (18). We assume independence between any of the high-risk factors and pregnancy, and further assume that half the population are women.

Estimating high-risk proportions for children. Since the 500 Cities Project only reports data for adults 18 years and older, we take a different approach to estimating the proportion of children at high risk for severe influenza. The two most prevalent risk factors for children are asthma and obesity; we also account for childhood diabetes, HIV and cancer.
From Miller et al. (19), we obtain national estimates of chronic conditions in children. For asthma, we assume that variation among cities will be similar for children and adults. Thus, we use the relative prevalences of asthma in adults to scale our estimates for children in each city. The prevalence of HIV and cancer in children are taken from CDC HIV surveillance report (15) and cancer research report (20), respectively.

We first estimate the proportion of children having either asthma, diabetes, cancer or HIV (assuming no overlap in these conditions). We estimate city-level morbid obesity in children using the estimated morbid obesity in adults multiplied by a national constant ratio for each age group estimated from Hales et al. (21), this ratio represents the prevalence in morbid obesity in children given the one observed in adults. From Morgan et al. (17), we estimate that 25% of morbidly obese children have another high-risk condition and adjust our final estimates accordingly.

Resulting estimates. We compare our estimates for the Austin-Round Rock Metropolitan Area to published national-level estimates (22) of the proportion of each age group with underlying high risk conditions (Table A6). The biggest difference is observed in older adults, with Austin having a lower proportion at risk for complications for COVID-19 than the national average; for 25-39 year olds the high risk proportion is slightly higher than the national average.

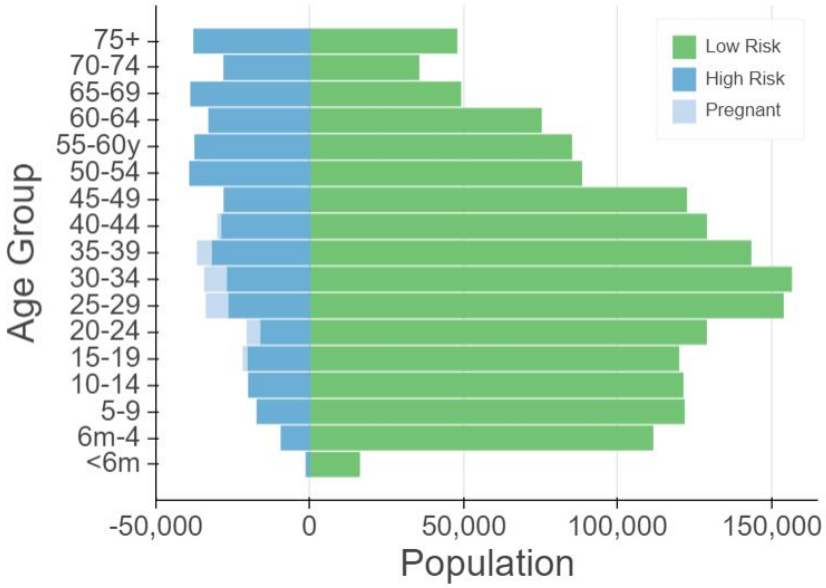

Figure A3. Demographic and risk composition of the Austin-Round Rock MSA. Bars indicate age-specific population sizes, separated by low risk, high risk, and pregnant. High risk is defined as individuals with cancer, chronic kidney disease, COPD, heart disease, stroke, asthma, diabetes, HIV/AIDS, and morbid obesity, as estimated from the CDC 500 Cities Project (12), reported HIV prevalence (15) and reported morbid obesity prevalence (16,17), corrected for multiple conditions. The population of pregnant women is derived using the CDC's method combining fertility, abortion and fetal loss rates (23–25).

Table A7. High-risk conditions for influenza and data sources for prevalence estimation

Condition	Data source
Cancer (except skin), chronic kidney disease, COPD, coronary heart disease, stroke, asthma, diabetes	CDC 500 cities (12)
HIV/AIDS	CDC HIV Surveillance report (15)
Obesity	CDC 500 cities (12), Sturm and Hattori (16), Morgan et al. (17)
Pregnancy	National Vital Statistics Reports (23) and abortion data (24)

Table A8: Comparison between published national estimates and Austin-Round Rock MSA estimates of the percent of the population at high-risk of influenza/COVID-19 complications.

Age Group	National estimates (21)	Austin (excluding pregnancy)	Pregnant women (proportion of age group)
0 to 6 months	NA	6.8	-
6 months to 4 years	6.8	7.4	-
5 to 9 years	11.7	11.6	-
10 to 14 years	11.7	13.0	-
15 to 19 years	11.8	13.3	1.7
20 to 24 years	12.4	10.3	5.1
25 to 34 years	15.7	13.5	7.8
35 to 39 years	15.7	17.0	5.1
40 to 44 years	15.7	17.4	1.2
45 to 49 years	15.7	17.7	-
50 to 54 years	30.6	29.6	-
55 to 60 years	30.6	29.5	-
60 to 64 years	30.6	29.3	-
65 to 69 years	47.0	42.2	-
70 to 74 years	47.0	42.2	-
75 years and older	47.0	42.2	-

References

1. Keeling MJ, Rohani P. Modeling Infectious Diseases in Humans and Animals. Princeton University Press; 2011. 408 p.

2. Gillespie DT. Approximate accelerated stochastic simulation of chemically reacting systems. J Chem Phys. 2001 Jul 22;115(4):1716–33.

3. scipy.optimize.least_squares — SciPy v1.4.1 Reference Guide [Internet]. [cited 2020 Apr 26]. Available from: https://docs.scipy.org/doc/scipy/reference/generated/scipy.optimize.least_squares.html

4. Verity R, Okell LC, Dorigatti I, Winskill P, Whittaker C, Imai N, et al. Estimates of the severity of COVID-19 disease [Internet]. Epidemiology. medRxiv; 2020. Available from: https://www.medrxiv.org/content/10.1101/2020.03.09.20033357v1.abstract

5. Mizumoto K, Kagaya K, Zarebski A, Chowell G. Estimating the Asymptomatic Proportion of 2019 Novel Coronavirus onboard the Princess Cruises Ship, 2020 [Internet]. Infectious Diseases (except HIV/AIDS). medRxiv; 2020. Available from: https://www.medrxiv.org/content/10.1101/2020.02.20.20025866v2

6. Lauer SA, Grantz KH, Bi Q, Jones FK, Zheng Q, Meredith HR, et al. The Incubation Period of Coronavirus Disease 2019 (COVID-19) From Publicly Reported Confirmed Cases: Estimation and Application. Ann Intern Med [Internet]. 2020 Mar 10; Available from: http://dx.doi.org/10.7326/M20-0504

7. Du Z, Xu X, Wu Y, Wang L, Cowling BJ, Meyers LA. The serial interval of COVID-19 from publicly reported confirmed cases [Internet]. Epidemiology. medRxiv; 2020. Available from: https://www.medrxiv.org/content/10.1101/2020.02.19.20025452v3

8. CDC. People at High Risk of Flu [Internet]. Centers for Disease Control and Prevention. 2019 [cited 2020 Mar 26]. Available from: https://www.cdc.gov/flu/highrisk/index.htm

9. CDC - BRFSS [Internet]. 2019 [cited 2020 Mar 26]. Available from: https://www.cdc.gov/brfss/index.html

10. Zhang X, Holt JB, Lu H, Wheaton AG, Ford ES, Greenlund KJ, et al. Multilevel regression and poststratification for small-area estimation of population health outcomes: a case study of chronic obstructive pulmonary disease prevalence using the behavioral risk factor surveillance system. Am J Epidemiol. 2014 Apr 15;179(8):1025–33.

11. Tindale L, Coombe M, Stockdale JE, Garlock E, Lau WYV, Saraswat M, et al. Transmission interval estimates suggest pre-symptomatic spread of COVID-19 [Internet]. Epidemiology. medRxiv; 2020. Available from: http://dx.doi.org/10.1101/2020.03.03.20029983

12. 500 Cities Project: Local data for better health | Home page | CDC [Internet]. 2019 [cited 2020 Mar 19]. Available from: https://www.cdc.gov/500cities/index.htm

13. Health Outcomes | 500 Cities [Internet]. 2019 [cited 2020 Mar 28]. Available from:

https://www.cdc.gov/500cities/definitions/health-outcomes.htm

14. Part One: Who Lives with Chronic Conditions [Internet]. Pew Research Center: Internet, Science & Tech. 2013 [cited 2019 Nov 23]. Available from: https://www.pewresearch.org/internet/2013/11/26/part-one-who-lives-with-chronic-conditions/

15. for Disease Control C, Prevention, Others. HIV surveillance report. 2016; 28. URL: http://www cdc gov/hiv/library/reports/hiv-surveil-lance html Published November. 2017;

16. Sturm R, Hattori A. Morbid obesity rates continue to rise rapidly in the United States. Int J Obes . 2013 Jun;37(6):889–91.

17. Morgan OW, Bramley A, Fowlkes A, Freedman DS, Taylor TH, Gargiullo P, et al. Morbid obesity as a risk factor for hospitalization and death due to 2009 pandemic influenza A(H1N1) disease. PLoS One. 2010 Mar 15;5(3):e9694.

18. Estimating the Number of Pregnant Women in a Geographic Area from CDC Division of Reproductive Health. Available from: https://www.cdc.gov/reproductivehealth/emergency/pdfs/PregnacyEstimatoBrochure508.pdf

19. Miller GF, Coffield E, Leroy Z, Wallin R. Prevalence and Costs of Five Chronic Conditions in Children. J Sch Nurs. 2016 Oct;32(5):357–64.

20. Cancer Facts & Figures 2014 [Internet]. [cited 2020 Mar 30]. Available from: https://www.cancer.org/research/cancer-facts-statistics/all-cancer-facts-figures/cancer-facts-figures-2014.html

21. Hales CM, Fryar CD, Carroll MD, Freedman DS, Ogden CL. Trends in Obesity and Severe Obesity Prevalence in US Youth and Adults by Sex and Age, 2007-2008 to 2015-2016. JAMA. 2018 Apr 24;319(16):1723–5.

22. Zimmerman RK, Lauderdale DS, Tan SM, Wagener DK. Prevalence of high-risk indications for influenza vaccine varies by age, race, and income. Vaccine. 2010 Sep 7;28(39):6470–7.

23. Martin JA, Hamilton BE, Osterman MJK, Driscoll AK, Drake P. Births: Final Data for 2017. Natl Vital Stat Rep. 2018 Nov;67(8):1–50.

24. Jatlaoui TC, Boutot ME, Mandel MG, Whiteman MK, Ti A, Petersen E, et al. Abortion Surveillance - United States, 2015. MMWR Surveill Summ. 2018 Nov 23;67(13):1–45.

25. Ventura SJ, Curtin SC, Abma JC, Henshaw SK. Estimated pregnancy rates and rates of pregnancy outcomes for the United States, 1990-2008. Natl Vital Stat Rep. 2012 Jun 20;60(7):1–21.